Expresión génica diferencial en desarrollo

MÓDULO 3, BIOLOGÍA DEL DESARROLLO

JOAGARAT@GMAIL.COM

Informe

Formato:

-Introducción

-Materiales y métodos

-Resultados

Máximo 3 carillas

-Bibliografía

-Anexo (Figuras)

Recordemos un poco…

¿En qué consiste un experimento de RNAseq?

¿Qué resultados nos permite obtener?

¿Qué se imaginan que varía en un experimento de single cell RNAseq respecto a un experimento de RNAseq tradicional?

Objetivo de este práctico

Visualizar y re-analizar un set de datos de transcriptómica de célula única proveniente de embriones de ratón en diferentes estadios del desarrollo, familiarizándonos con este tipo de datos y observando cómo varia la expression génica durante la organogénesis.

Introducción a transcriptómica de célula única (single cell RNAseq)

average expression level

- comparative transcriptomics
- disease biomarker
- homogenous systems

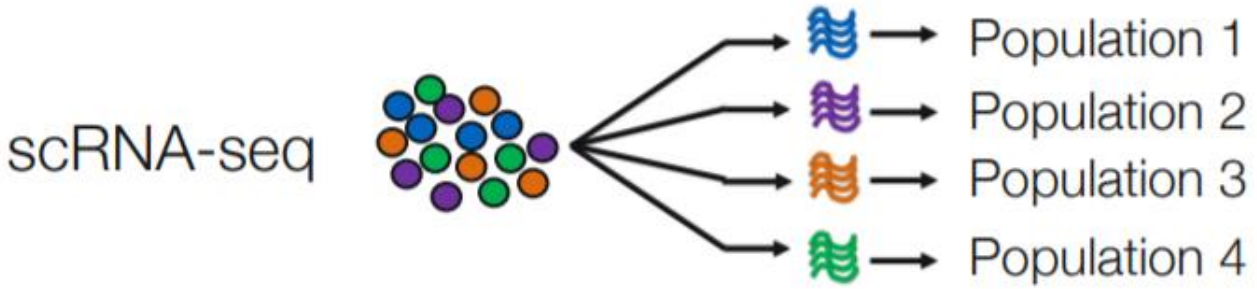

- define heterogeneity
- identify rare cell population
- cell population dynamics

Aplicaciones de single cell RNAseq

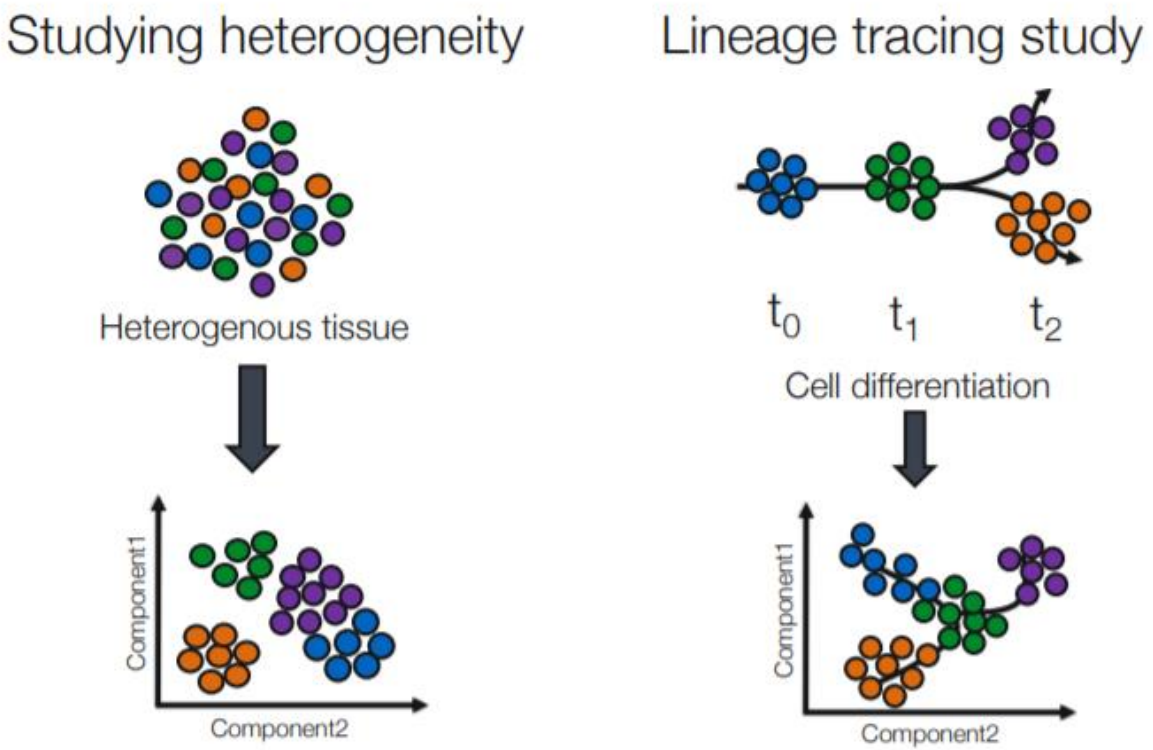

Artículos de single cell RNAseq

Single-Cell RNA-Seq of the Developing Cardiac Outflow Tract Reveals Convergent Development of the Vascular Smooth Muscle Cells

Xuanyu Liu [1], Wen Chen [1], Wenke Li [1], Yan Li [2], James R Priest [3], Bin Zhou [4], Jikui Wang [5], Zhou Zhou [6]

Affiliations + expand

PMID: 31365875 DOI: 10.1016/j.celrep.2019.06.092

Free article

Abstract

Cardiac outflow tract (OFT) is a major hotspot for congenital heart diseases. A thorough understanding of the cellular diversity, transitions, and regulatory networks of normal OFT development is essential to decipher the etiology of OFT malformations. We performed single-cell transcriptomic sequencing of 55,611 mouse OFT cells from three developmental stages that generally correspond to the early, middle, and late stages of OFT remodeling and septation. Known cellular transitions, such as endothelial-to-mesenchymal transition, have been recapitulated. In particular, we identified convergent development of the vascular smooth muscle cell (VSMC) lineage where intermediate cell subpopulations were found to be involved in either myocardial-to-VSMC trans-differentiation or mesenchymal-to-VSMC transition. Finally, we uncovered transcriptional regulators potentially governing cellular transitions. Our study provides a single-cell reference map of cell states for normal OFT development and paves the way for further studies of the etiology of OFT malformations at the single-cell level.

cells from limited samples. Currently, the widespread application of single-cell RNA sequencing technology is gradually changing our understanding of disease pathogenesis. This article reviews the application of single-cell RNA sequencing in embryonic development in recent years and provides innovative ideas for research on embryonic development and the treatment of diseases related to embryonic development.

Understanding development and stem cells using single cell-based analyses of gene expression

Pavithra Kumar, Yuqi Tan, Patri

Development 2017 144: 17-32;

Article | Figures & tables

Abstract

Single-cell RNA sequencing disease

S. Steven Potter

Author information · Copyright and Lic

The publisher's final edited version of this
See other articles in PMC that cite the pu

An ongoing technological revolution is
studies of gene expression patterns. Cur
single cells to be defined, facilitating dis
hidden. In contrast to gene expression st
average of the diverse constituent cells,
within a complex population mix, such
expression profiling has contributed to i
cells make different differentiation decis
expression studies have enabled the cha
and facilitated the identification of nove
understanding of both normal and disea
of new treatment approaches. Although
single-cell gene expression patterns is ir
gene expression patterns of all cell types

Sci Adv. 2020 Aug 21;6(34):eaaz2978. doi: 10.1126/sciadv.aaz2978. eCollection 2020 Aug.

Single-cell transcriptome analysis reveals cell lineage specification in temporal-spatial patterns in human cortical development

Xiaoying Fan [1 2 3], Yuanyuan Fu [4], Xin Zhou [3 5], Le Sun [3 5], Ming Yang [1 6], Mengdi Wang [5], Ruiguo Chen [3 5], Qian Wu [3 5], Jun Yong [1 6], Ji Dong [1 2], Lu Wen [1 2], Jie Qiao [1 6 7 8], Xiaoqun Wang [3 5 9], Fuchou Tang [1 2 8]

Affiliations + expand

PMID: 32923614 PMCID: PMC7450478 DOI: 10.1126/sciadv.aaz2978

Free PMC article

Abstract

Neurogenesis processes differ in different areas of the cortex in many species, including humans. Here, we performed single-cell transcriptome profiling of the four cortical lobes and pons during human embryonic and fetal development. We identified distinct subtypes of neural progenitor cells (NPCs) and their molecular signatures, including a group of previously unidentified transient NPCs. We specified the neurogenesis path and molecular regulations of the human deep-layer, upper-layer, and mature neurons. Neurons showed clear spatial and temporal distinctions, while glial cells of different origins showed development patterns similar to those of mice, and we captured the developmental trajectory of oligodendrocyte lineage cells until the human mid-fetal stage. Additionally, we verified region-specific characteristics of neurons in the cortex, including their distinct electrophysiological features. With systematic single-cell analysis, we decoded human neuronal development in temporal and spatial dimensions from GW7 to GW28, offering deeper insights into the molecular regulations underlying human neurogenesis and cortical development.

De dónde provienen los datos que vamos a analizar?

› Nature. 2019 Feb;566(7745):496-502. doi: 10.1038/s41586-019-0969-x. Epub 2019 Feb 20.

The single-cell transcriptional landscape of mammalian organogenesis

Junyue Cao [1 2], Malte Spielmann [1], Xiaojie Qiu [1 2], Xingfan Huang [1 3], Daniel M Ibrahim [4 5], Andrew J Hill [1], Fan Zhang [6], Stefan Mundlos [4 5], Lena Christiansen [6], Frank J Steemers [6], Cole Trapnell [7 8 9], Jay Shendure [10 11 12 13]

Affiliations + expand

PMID: 30787437 PMCID: PMC6434952 DOI: 10.1038/s41586-019-0969-x

Free PMC article

Abstract

Mammalian organogenesis is a remarkable process. Within a short timeframe, the cells of the three germ layers transform into an embryo that includes most of the major internal and external organs. Here we investigate the transcriptional dynamics of mouse organogenesis at single-cell resolution. Using single-cell combinatorial indexing, we profiled the transcriptomes of around 2 million cells derived from 61 embryos staged between 9.5 and 13.5 days of gestation in a single experiment. The resulting 'mouse organogenesis cell atlas' (MOCA) provides a global view of developmental processes during this critical window. We use Monocle 3 to identify hundreds of cell types and 56 trajectories, many of which are detected only because of the depth of cellular coverage, and collectively define thousands of corresponding marker genes. We explore the dynamics of gene expression within cell types and trajectories over time, including focused analyses of the apical ectodermal ridge, limb mesenchyme and skeletal muscle.

METHODS

Data reporting. No statistical methods were used to predetermine sample size. Embryos used in experiments were randomized before sample preparation. Investigators were blinded to group allocation during data collection and analysis: embryo collection and sci-RNA-seq3 analysis were performed by two different researchers.

Embryo dissection. The C57BL/6 mice were obtained from The Jackson Laboratory and plug matings were set up. Noon on the day of the vaginal plug was considered as E0.5. Dissections were performed as previously described[51] and all embryos were immediately snap-frozen in liquid nitrogen. Embryos were collected from at least three independent litters per development stage. All animal procedures were in accordance with institutional, state, and government regulations and approved by the Office of Animal Welfare (OAW) under the IACUC protocol 4378-01.

Mouse embryo nuclei extraction and fixation. Mouse embryos from different development stages were processed together to reduce batch effects. Each mouse embryo was minced into small pieces by blade in 1 ml ice-cold cell lysis buffer (10 mM Tris-HCl, pH 7.4, 10 mM NaCl, 3 mM MgCl2 and 0.1% IGEPAL CA-630[52], modified to also include 1% SUPERase In and 1% BSA (molecular biology grade, NEB, 20mg/ml)) and transferred to the top of a 40-μm cell strainer (Falcon). Tissues were homogenized with the rubber tip of a syringe plunger (5 ml, BD) in 4 ml cell lysis buffer. The filtered nuclei were then transferred to a new 15-ml tube (Falcon) and pelleted by centrifugation at 500*g* for 5 min and washed once with 1 ml cell lysis buffer. The nuclei were fixed in 4 ml ice cold 4% paraformaldehyde (EMS) for 15 min on ice. After fixation, the nuclei were washed twice in 1 ml nuclei wash buffer (cell lysis buffer without IGEPAL), and re-suspended in 500 μl nuclei wash buffer. The samples were split to 2 tubes with 250 μl in each tube and flash-frozen in liquid nitrogen. We estimated the nuclei extraction efficiency based on the extracted nuclei number versus expected total nuclei number in each embryo. The estimated nuclei extraction efficiency ranged from 60% to 85%.

Organogénesis en Ratón

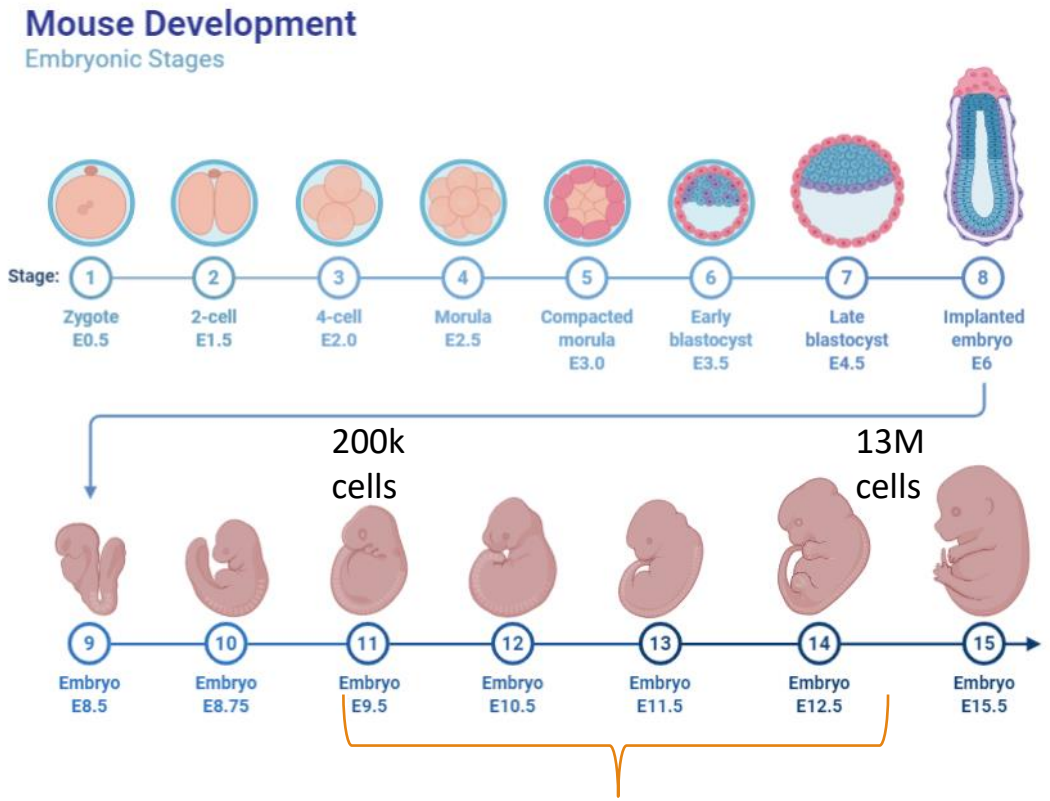

Etapas en las que los investigadores extraen células para estudiar organogénesis

Como obtuvieron los investigadores estos datos?

Análisis de resultados

Processing of sequencing reads. Base calls were converted to fastq format using Illumina's bcl2fastq/v.2.16 and demultiplexed based on PCR i5 and i7 barcodes using the maximum likelihood demultiplexing package deML[53] with default settings. Downstream sequence processing and single-cell digital-expression matrix generation were similar to sci-RNA-seq[17] except that reverse transcription index was combined with hairpin adaptor index, and thus the mapped reads were split into constituent cellular indices by demultiplexing reads using both the reverse transcription index and ligation index (Levenshtein edit distance (ED) < 2, including insertions and deletions). In brief, demultiplexed reads were filtered on the basis of the reverse transcription index and ligation index (ED <2, including insertions and deletions) and adaptor-clipped using trim_galore v.0.4.1 with default settings. Trimmed reads were mapped to the mouse reference genome (mm10) for mouse embryo nuclei, or a chimeric reference genome of human hg19 and mouse mm10 for HEK-293T and NIH/3T3 mixed nuclei, using STAR v.2.5.2b[54] with default settings and gene annotations (GENCODE V19 for human; GENCODE VM11 for mouse). Uniquely mapping reads were extracted, and duplicates were removed using the unique molecular identifier (UMI) sequence, reverse transcription index, hairpin ligation adaptor index and read 2 end-coordinate (that is, reads with identical UMI, reverse transcription index, ligation adaptor index and tagmentation site were considered duplicates). Finally, mapped reads were split into constituent cellular indices by further demultiplexing reads using the reverse transcription index and ligation hairpin (ED <2, including insertions and deletions). For mixed-species experiment, the percentage of uniquely mapping

cells classified as mixed cells or 'collisions'. To generate digital expression matrices, we calculated the number of strand-specific UMIs for each cell mapping to the exonic and intronic regions of each gene with the Python v.2.7.13 HTseq package[55]. For multi-mapped reads, reads were assigned to the closest gene, except in cases in which another intersected gene fell within 100 bp of the end of the closest gene, in which case the read was discarded. For most analyses, we included both expected-strand intronic and exonic UMIs in per-gene single-cell expression matrices.

Whole-mouse embryo analysis. After the single-cell gene count matrix was generated, each cell was assigned to its original mouse embryo on the basis of the reverse transcription barcode. Reads mapping to each embryo were aggregated to generate 'bulk RNA-seq' for each embryo. For sex separation of embryos, we counted reads mapping to a female-specific non-coding RNA (*Xist*) or chrY genes (except *Erdr1* which is in both chrX and chrY). Embryos were readily separated into females (more reads mapping to *Xist* than chrY genes) and males (more reads mapping to chrY genes than *Xist*).

Pseudotemporal ordering of whole-mouse embryos was done using Monocle 2[56]. In brief, an aggregated gene-expression matrix was constructed as described above. Differentially expressed genes across different development conditions were identified with the differentialGeneTest function of Monocle 2[56]. The top 2,000 genes with the lowest q value were used to construct the pseudotime trajectory using Monocle 2[56]. Each embryo was assigned a pseudotime value on the basis of its position along the trajectory.

Opciones

Data availability

The sci-RNA-seq3 protocol and all data have been made freely available, including through a cell-type wiki to facilitate their ongoing annotation by the research community (http://atlas.gs.washington.edu/mouse-rna). The data generated in this study can be downloaded in raw and processed forms from the NCBI Gene Expression Omnibus under accession number GSE119945.

1)

- Descargar las 11.000.000.000 de secuencias
- Filtrar por calidad y alinearlas contra el genoma
- Generar una matríz de conteos
- Utilizar herramientas bioinformáticas complejas específicas para este tipo de análisis.

Necesidad de altísima capacidad computacional y de formación en bioinformática

2)

- Visualizar y analizar los resultados en el atlas web publicado por los investigadores.

https://descartes.brotmanbaty.org/

descartes

Divide each difficulty into as many parts as is feasible and necessary to resolve it.

Human
Gene Expression
During Development

4M Cells | 121 Tissues | 15 Organs

ATLAS | PUBLICATION

Human
Chromatin Accessibility
During Development

720K Cells | 53 Tissues | 15 Organs

ATLAS | PUBLICATION

Mammalian
Organogenesis

~2M Cells | 61 Embryos

ATLAS | PUBLICATION

Mouse
Chromatin Accessibility

~100K Cells | 13 Tissues

ATLAS | PUBLICATION

Worm
Gene Expression

~49K Cells

ATLAS | PUBLICATION

Fly
Chromatin Accessibility

~23K Cells | 3 Timepoints

ATLAS | PUBLICATION

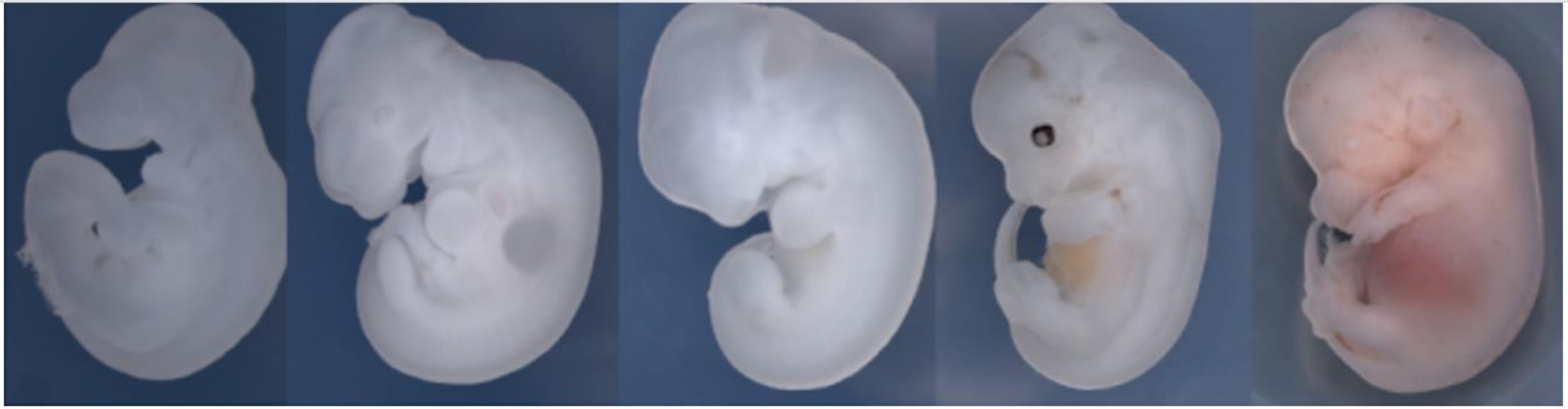

In our manuscript (Cao, J. and Spielmann, M. et al.), we profiled ~2 million cells, derived from 61 embryos staged between 9.5 and 13.5 days of gestation, in a single experiment. We identify hundreds of cell types and 56 trajectories, and collectively define thousands of corresponding marker genes and dynamics of gene expression within cell types and trajectories over time.

Trajectories

Explore our cell trajectories and subtrajectories in 3D UMAP space.

Explore Trajectories

Clusters

Explore our cell clusters and subclusters in t-SNE space.

Explore Clusters

Genes

Search for the expression of a gene in cell clusters and subclusters.

Search Genes

Data Sets

We have made our primary and secondary data available for the research community along with extensive documentation.

Download Data

sci-RNA-seq3

To generate these data, we used a novel high throughput single cell RNA-seq technique called sci-RNA-seq3, which can profile millions of cells in a single experiment. sci-RNA-seq3 is an upgraded version of sci-RNA-seq, and is based on a methodological framework called combinatorial indexing to profile millions of cells or nuclei without single cell isolation.

Learn More

Video

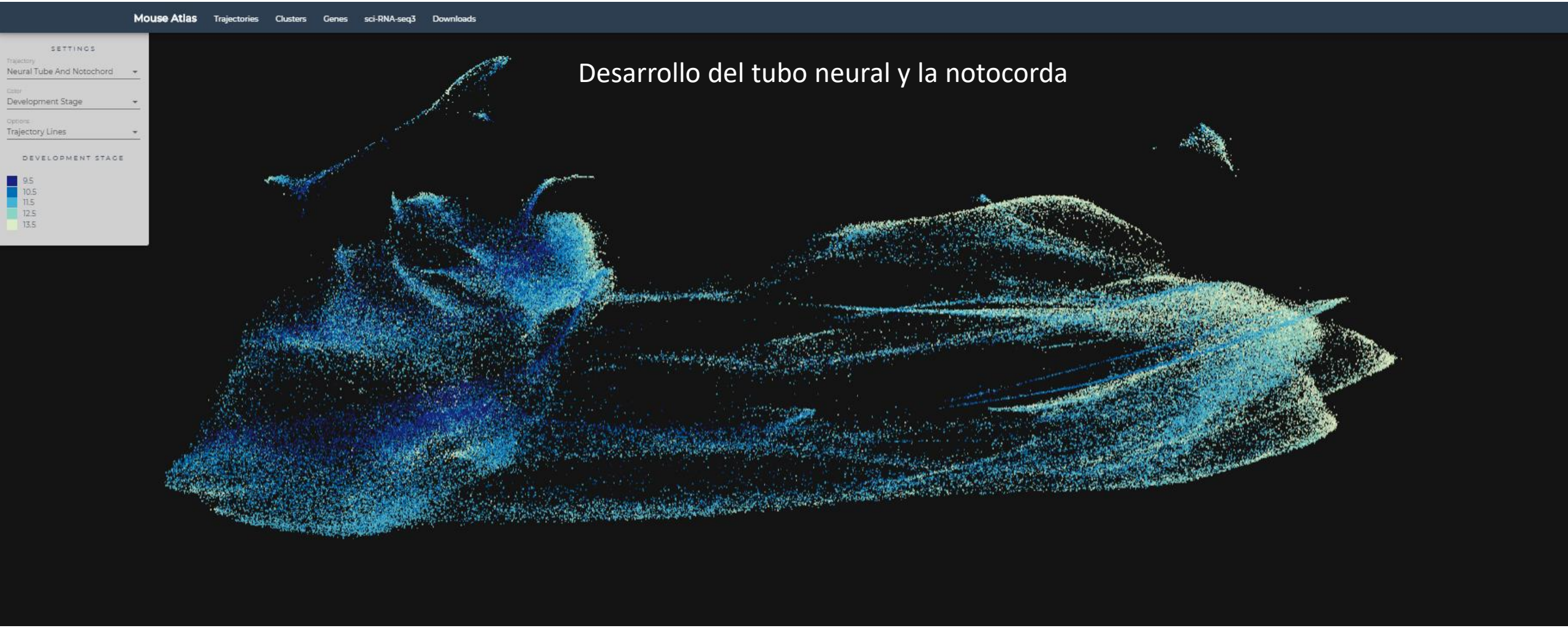
Mouse Atlas
Trajectories
Clusters
Genes
sci-RNA-seq3
Downloads
SETTINGS
Trajectory
Neural Tube And Notochord
Color
Development Stage
Options
Trajectory Lines
DEVELOPMENT STAGE
9.5
10.5
11.5
12.5
13.5
Desarrollo del tubo neural y la notocorda

Qué tipos celulares hay en cada estadio?

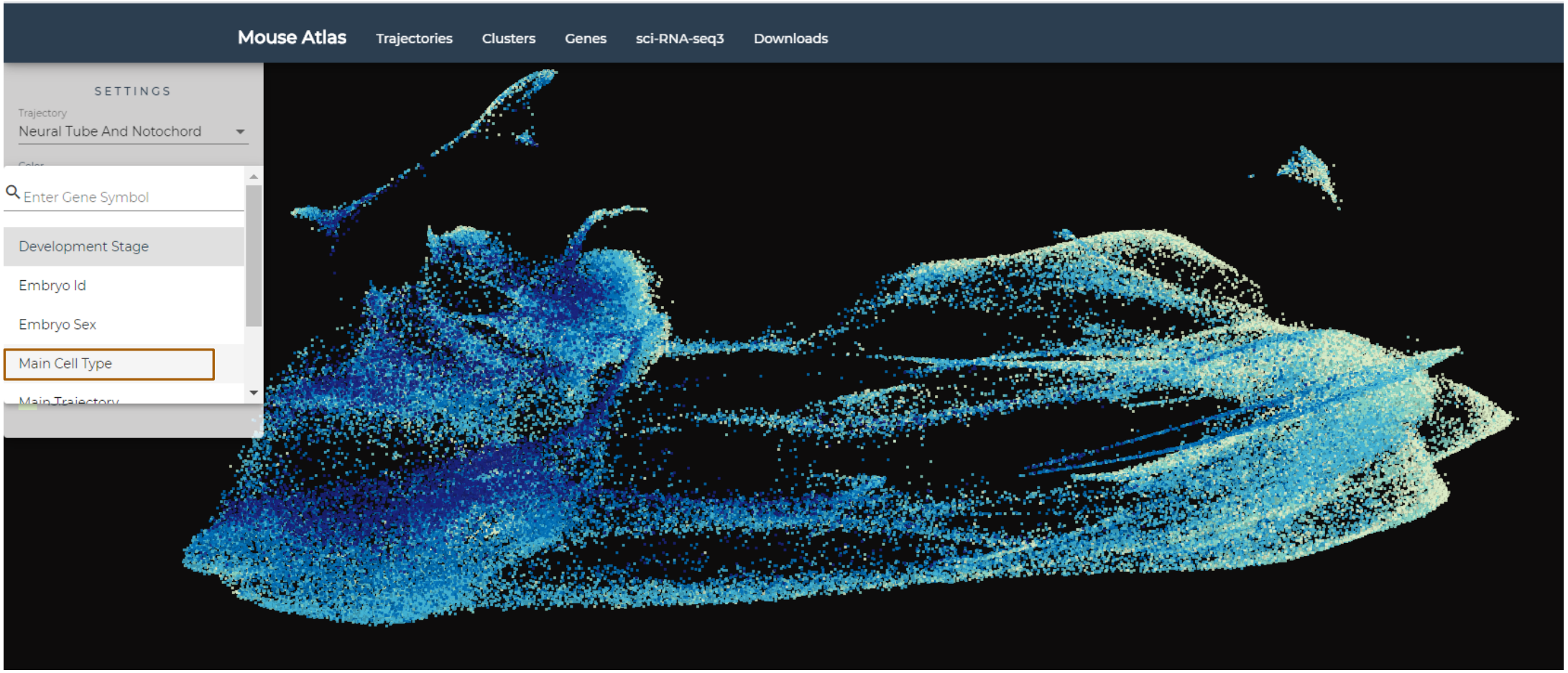

Mouse Atlas Trajectories Clusters Genes sci-RNA-seq3 Downloads

SETTINGS

Trajectory
Neural Tube And Notochord

Color
Main Cell Type

Options
Trajectory Lines

MAIN CELL TYPE

- Cardiac muscle lineages
- Cholinergic neurons
- Chondroctye progenitors
- Chondrocytes & osteoblasts
- Connective tissue progenitors
- Definitive erythroid lineage
- Early mesenchyme
- Endothelial cells
- Ependymal cell
- Epithelial cells
- Excitatory neurons
- Granule neurons
- Hepatocytes
- Inhibitory interneurons

Neuronas excitatorias

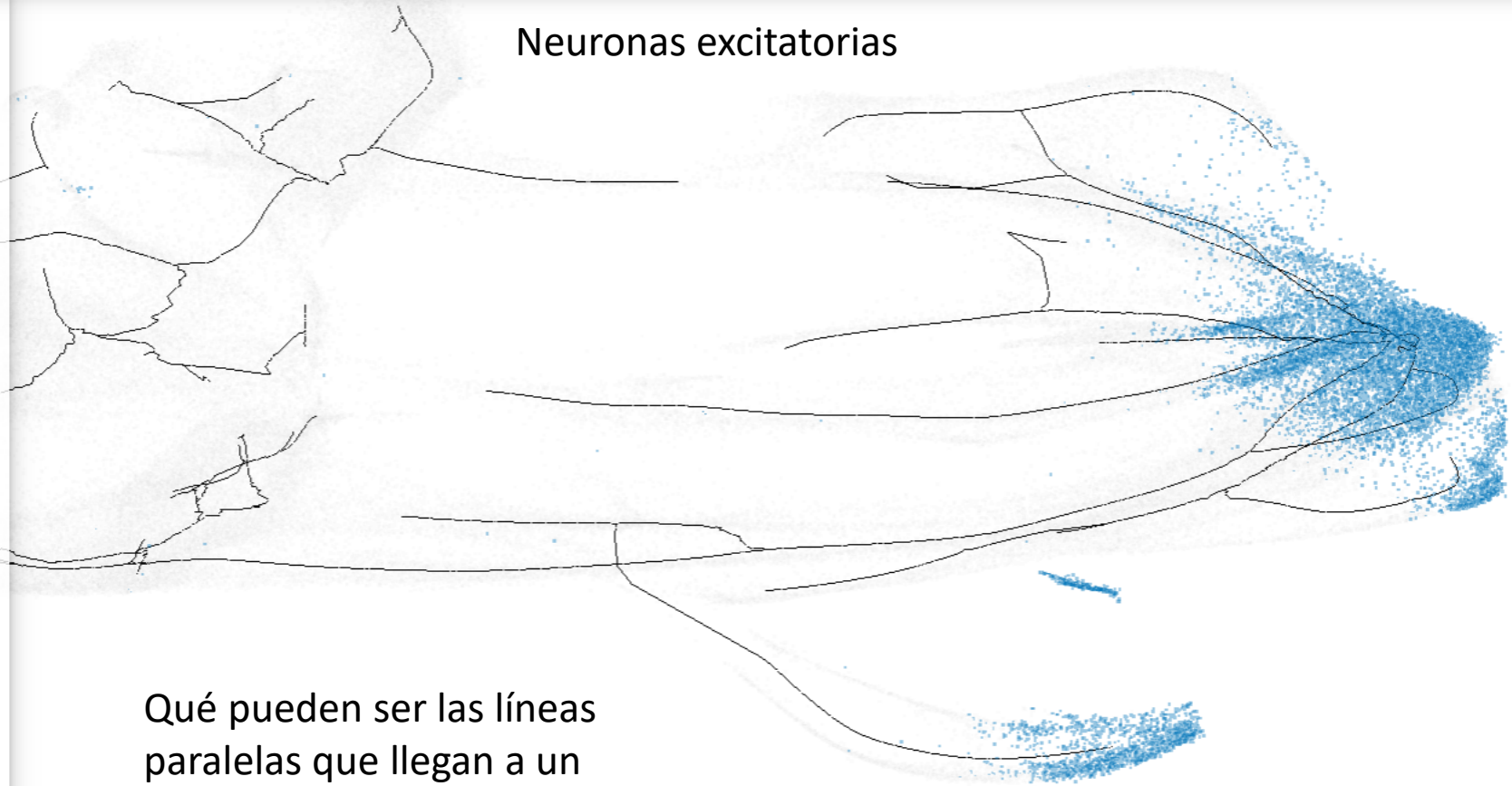

Qué pueden ser las líneas paralelas que llegan a un mismo destino?

Progenitores neuronales

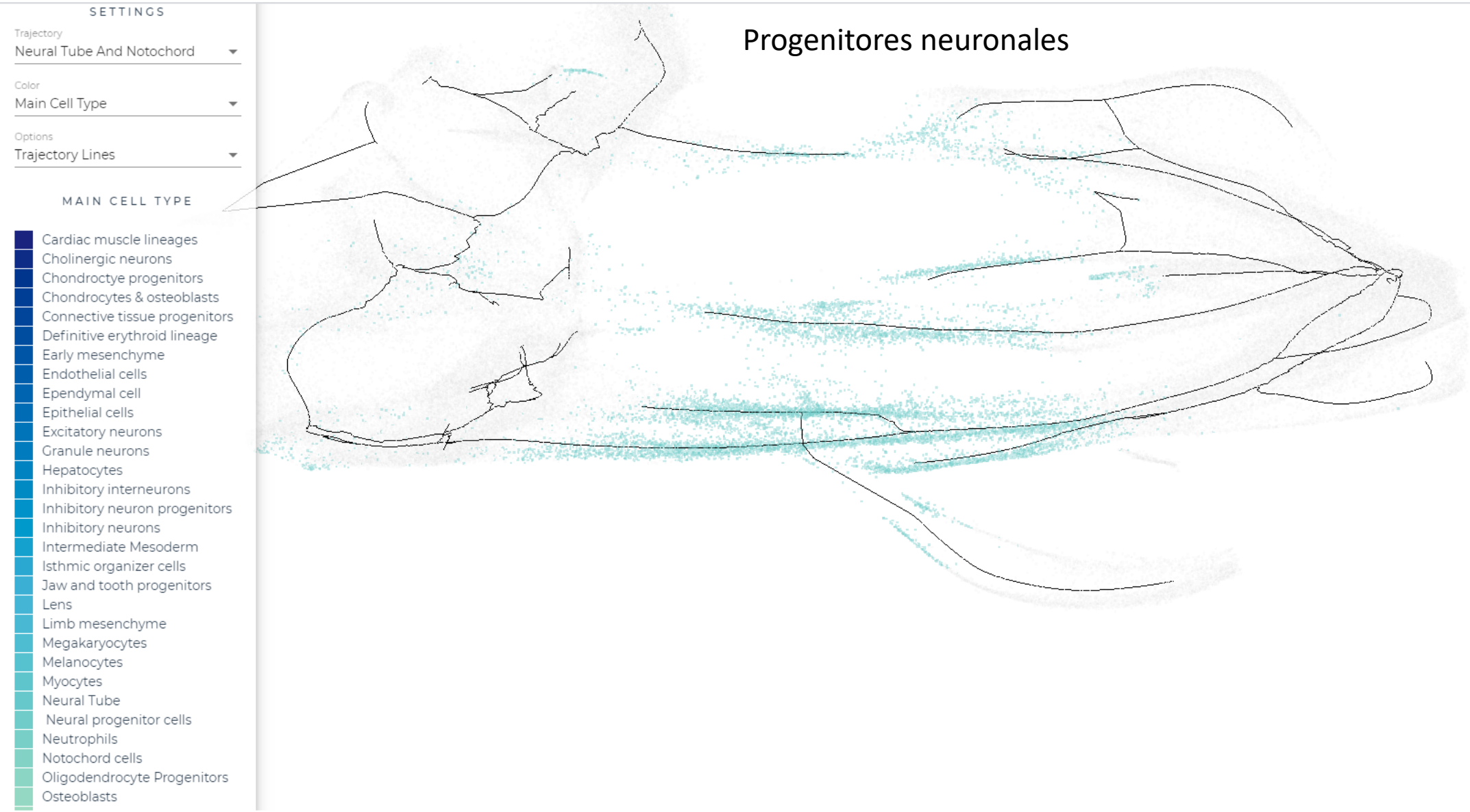

Se puede detectar los marcadores genéticos de cada cluster detectado.
Cómo varia el número de células detectado a medida que se avanza en el desarrollo?

Mouse Atlas | Trajectories | Clusters | Genes | sci-RNA-seq3 | Downloads

Cell Type: Neural Tube

T-SNE Cluster: Main Cluster

Filter Table

Gene ID	Gene Name	Gene Type	P Value	Q Value	Fold Change	Max Expression	Max Cluster	Second Cluster
ENSMUSG00000059246.4	Foxb1	protein coding	6.39e-52	3.37e-51	2.72	60	14	12
ENSMUSG00000020083.13	2010107G23Rik	protein coding	0.0000207	0.0000407	2.41	11.8	14	5
ENSMUSG00000030432.12	Rpl28	protein coding	0.0176	0.0268	2.39	6.71	14	8
ENSMUSG00000089707.1	Slain1os	antisense	0.000135	0.00025	2.38	8.72	14	5
ENSMUSG00000027996.13	Sfrp2	protein coding	5.18e-277	8.45999999999999e-276	2.17	321	14	7
ENSMUSG00000097526.1	Gm26847	lincRNA	0.00347	0.00568	2.02	7.98	14	11
ENSMUSG00000064734.1	Gm23445	snRNA	0.000129	0.000241	1.94	7.2	14	9
ENSMUSG00000111090.1	RP23-331E5.9	TEC	0.00805	0.0127	1.9	6.38	14	16
ENSMUSG00000036030.9	Prtg	protein coding	0	0	1.89	1990	14	8
ENSMUSG00000097258.1	Gm26767	lincRNA	1.2e-20	3.98e-20	1.83	26.2	14	9
ENSMUSG00000041075.8	Fzd7	protein coding	1.14e-92	8.56e-92	1.78	131	14	16
ENSMUSG00000007279.14	Scube2	protein coding	0	0	1.77	336	14	7
ENSMUSG00000090534.1	Gm4675	processed transcript	2.28e-18	7.17e-18	1.77	18.7	14	30

Qué hace Foxb1?

64,192 Cells in Neural Tube

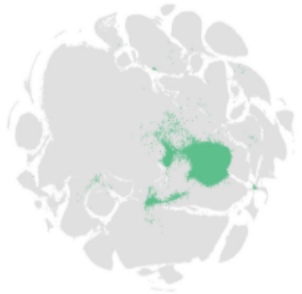

E9.5 | E10.5 | E11.5 | E12.5 | E13.5

Comments | Community | Login

Recommend | Sort by Best

Start the discussion...

LOG IN WITH

OR SIGN UP WITH DISQUS

Name

Ejercicio

Seleccione clusters celulares que le interesen y estén relacionados entre sí de cierta manera en el desarrollo (ej: notocorda, tubo neural, progenitores neurales, neuronas excitatorias)

Anote los marcadores más significativos

Esperaba la presencia de alguno de estos marcadores?

Encontró algún marcador que no esperaba?

Qué función cumplen estos genes?

Cómo le parece que afecta la expresión de este gen en el desarrollo?

Mouse Atlas | Trajectories | Clusters | Genes

Cell Type: Neural Progenitor Cells

T-SNE Cluster: Main Cluster

Gene ID	Gene Name	Gene Type	P Value
ENSMUSG00000025912.16	Mybl1	protein coding	1.11e-118
ENSMUSG00000021453.2	Gadd45g	protein coding	5.41e-76
ENSMUSG00000003436.11	Dll3	protein coding	0
ENSMUSG00000006649.17	Nphs1	protein coding	1.35e-33
ENSMUSG00000097767.8	Miat	lincRNA	0
ENSMUSG00000030350.8	Prmt8	protein coding	0
ENSMUSG00000067879.3	3110035E14Rik	protein coding	2.61e-42
ENSMUSG00000017692.8	Rhbdl3	protein coding	0
ENSMUSG00000097986.2	Gm26953	lincRNA	1.86e-62
ENSMUSG00000068154.5	Insm1	protein coding	6.65e-38
ENSMUSG00000103991.1	Gm38031	TEC	2.54e-8
ENSMUSG00000000202.9	Btbd17	protein coding	5.93e-125
ENSMUSG00000005089.15	Slc1a2	protein coding	0

ELSEVIER

Mechanisms of Development

Volume 128, Issues 7–10, September–December 2011, Pages 401-411

Gadd45a and *Gadd45g* regulate neural development and exit from pluripotency in *Xenopus*

Lilian T. Kaufmann [a], Christof Niehrs [a, b]

Show more

https://doi.org/10.1016/j.mod.2011.08.002

Abstract

Gadd45 genes encode a small family of multifunctional stress response proteins, mediating cell proliferation, apoptosis, DNA repair and DNA demethylation. Their role during embryonic development is incompletely understood. Here we identified

Teniendo en mente genes claves…

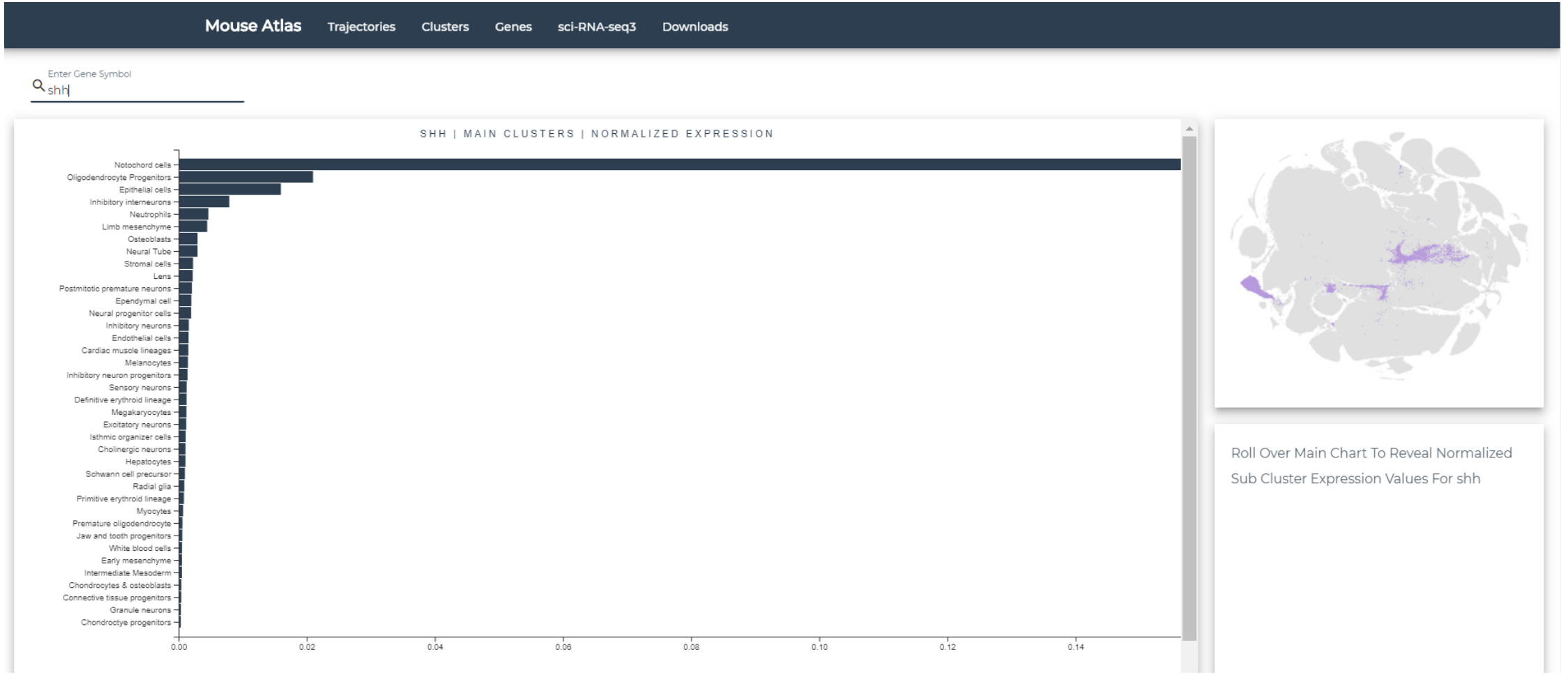

Recordemos…

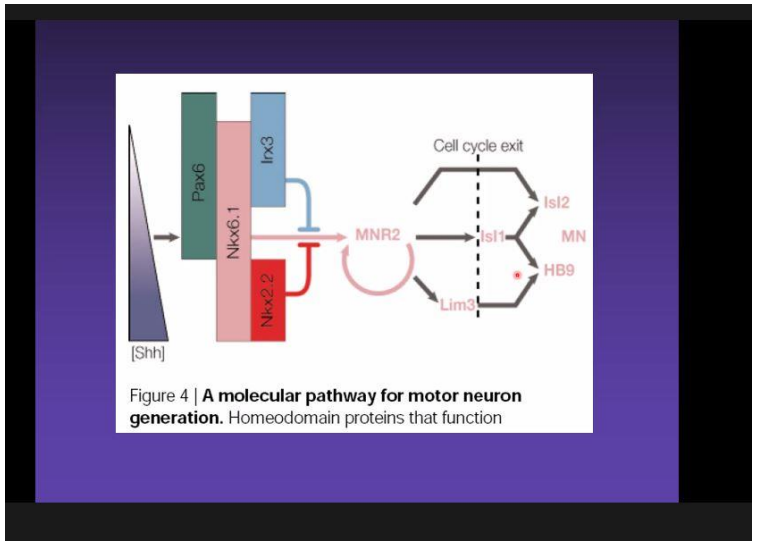

Figure 4 | **A molecular pathway for motor neuron generation.** Homeodomain proteins that function

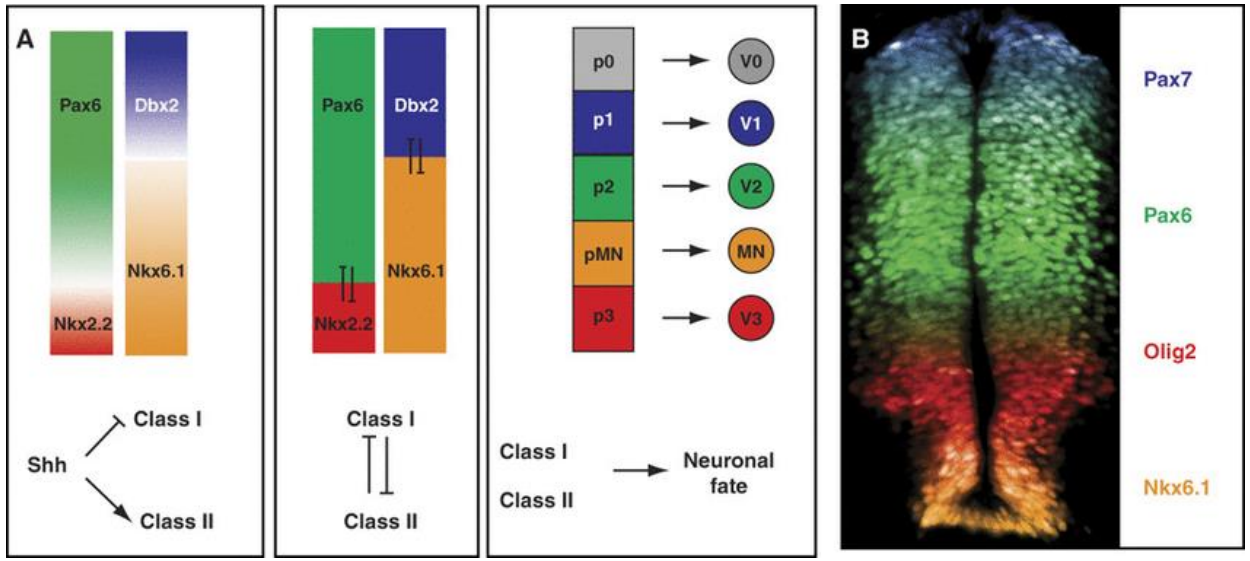

Ejercicio

Observen la expresión de genes claves en el desarrollo neuronal…

Cómo varia entre los principales tipos celulares?

Qué opina de la variación intra-tipo celular?

Considera que algún subcluster del tubo neural es más probable que contenga células de la región ventral? Y de la región dorsal?

Qué subcluster del tubo neural considera que es más probable que contenga a los precursores de motoneuronas?

Descarga y análisis de genes diferenciales

Differentially Expressed Gene List

We performed DE gene analysis to identify differentially expressed genes across 38 main cell types/10 main trajectories/56 sub-trajectories. We thend idenfied genes that are differentially expressed across sub-clusters within each main cluster. For each main trajectory and sub-trajectory, we identified genes that are differentially expressed across five development stages (from E9.5 to E13.5).

DE gene analysis result is stored in csv file. For each gene, the “max.cluster” is the group id with the highest expression (“max.expr”). The “second.cluster” is the group id with the second highest expression (“second.expr”). The “fold.change” is the fold change between the max expression and second max expression. The “qval” is the false detection rate (one-sided likelihood ratio test with multiple comparisons adjusted) for the gene differential expression test across different cell groups.

File name	Description	Modified	Details
DE_gene_main_cluster.csv	DE gene analysis result to identify differentially expressed genes across the 38 main clusters by main cluster ID (2.8M)	2018-12-05	Column name is explained above.
DE_gene_main_trajectory.csv	DE gene analysis result to identify differentially expressed genes across the ten main trajectories (6.5M)	2018-12-05	Column name is explained above.
DE_gene_sub_trajectory.csv	DE gene analysis result to identify differentially expressed genes across across 56 sub-trajectories (6.6M)	2018-12-05	Column name is explained above.
DE_gene_sub_cluster.tar.gz	DE gene analysis result to identify differentially expressed genes across sub-clusters within each main cluster by sub-cluster ID (28M)	2018-12-05	Each csv file is named by the main cluster ID.
main_trajectory_time.tar.gz	DE gene analysis result to identify differentially expressed genes across five development stages (E9.5 to E13.5) for each of the ten main trajectories (16M)	2018-12-05	Each csv file is named by the main trajectory ID encoded in the tra_name.csv file.
sub_trajectory_time.tar.gz	DE gene analysis result to identify differentially expressed genes across five development stages for each of the 56 sub-trajectories (77M)	2018-12-05	Each csv file is named by the sub-trajectory ID encoded in the tra_name.csv file.

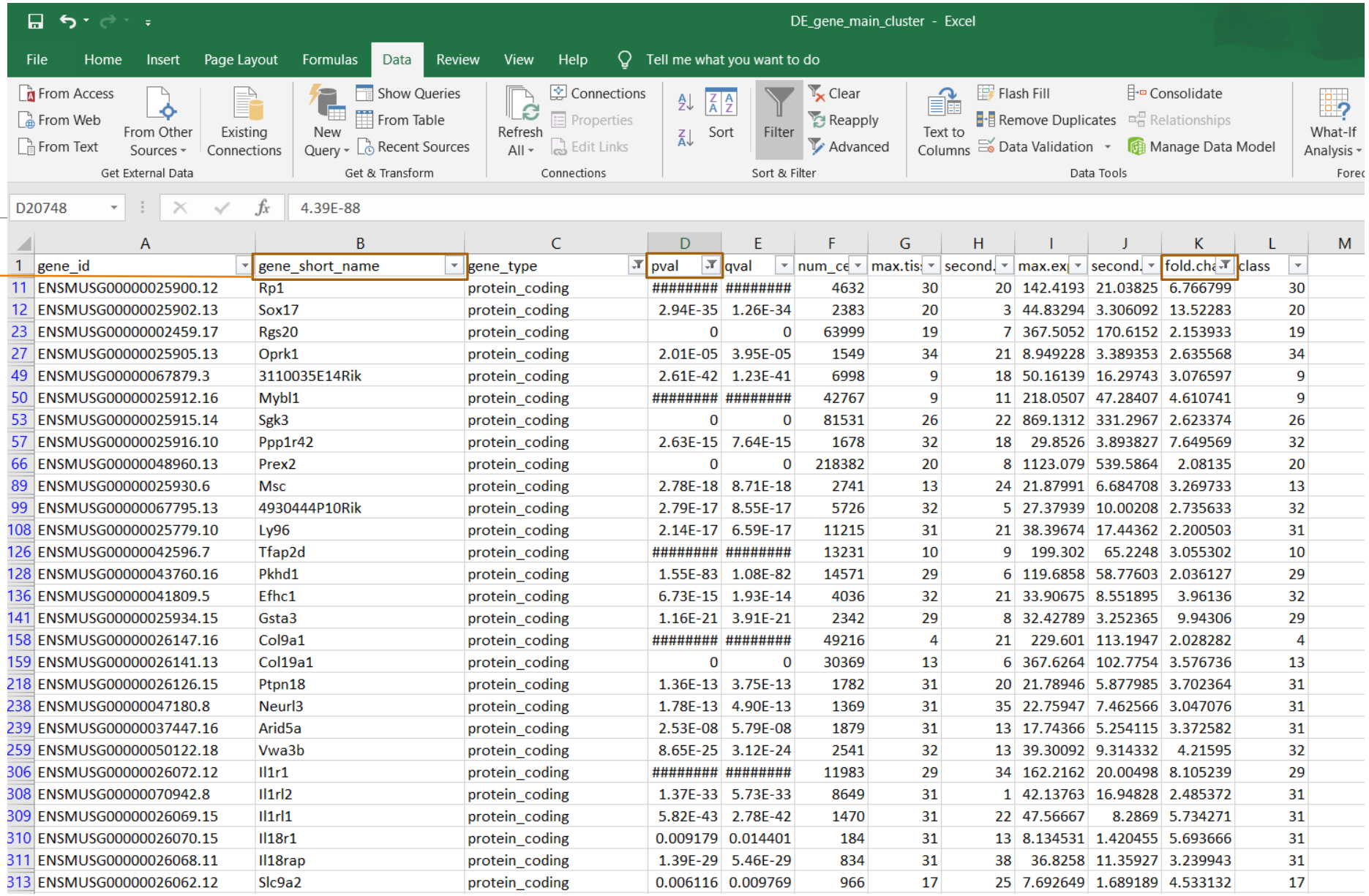

	A	B	C	D	E	F	G	H	I	J	K	L	M
1	gene_id	gene_short_name	gene_type	pval	qval	num_ce	max.tis	second.	max.ex	second.	fold.cha	class	
11	ENSMUSG00000025900.12	Rp1	protein_coding	########	########	4632	30	20	142.4193	21.03825	6.766799	30	
12	ENSMUSG00000025902.13	Sox17	protein_coding	2.94E-35	1.26E-34	2383	20	3	44.83294	3.306092	13.52283	20	
23	ENSMUSG00000002459.17	Rgs20	protein_coding	0	0	63999	19	7	367.5052	170.6152	2.153933	19	
27	ENSMUSG00000025905.13	Oprk1	protein_coding	2.01E-05	3.95E-05	1549	34	21	8.949228	3.389353	2.635568	34	
49	ENSMUSG00000067879.3	3110035E14Rik	protein_coding	2.61E-42	1.23E-41	6998	9	18	50.16139	16.29743	3.076597	9	
50	ENSMUSG00000025912.16	Mybl1	protein_coding	########	########	42767	9	11	218.0507	47.28407	4.610741	9	
53	ENSMUSG00000025915.14	Sgk3	protein_coding	0	0	81531	26	22	869.1312	331.2967	2.623374	26	
57	ENSMUSG00000025916.10	Ppp1r42	protein_coding	2.63E-15	7.64E-15	1678	32	18	29.8526	3.893827	7.649569	32	
66	ENSMUSG00000048960.13	Prex2	protein_coding	0	0	218382	20	8	1123.079	539.5864	2.08135	20	
89	ENSMUSG00000025930.6	Msc	protein_coding	2.78E-18	8.71E-18	2741	13	24	21.87991	6.684708	3.269733	13	
99	ENSMUSG00000067795.13	4930444P10Rik	protein_coding	2.79E-17	8.55E-17	5726	32	5	27.37939	10.00208	2.735633	32	
108	ENSMUSG00000025779.10	Ly96	protein_coding	2.14E-17	6.59E-17	11215	31	21	38.39674	17.44362	2.200503	31	
126	ENSMUSG00000042596.7	Tfap2d	protein_coding	########	########	13231	10	9	199.302	65.2248	3.055302	10	
128	ENSMUSG00000043760.16	Pkhd1	protein_coding	1.55E-83	1.08E-82	14571	29	6	119.6858	58.77603	2.036127	29	
136	ENSMUSG00000041809.5	Efhc1	protein_coding	6.73E-15	1.93E-14	4036	32	21	33.90675	8.551895	3.96136	32	
141	ENSMUSG00000025934.15	Gsta3	protein_coding	1.16E-21	3.91E-21	2342	29	8	32.42789	3.252365	9.94306	29	
158	ENSMUSG00000026147.16	Col9a1	protein_coding	########	########	49216	4	21	229.601	113.1947	2.028282	4	
159	ENSMUSG00000026141.13	Col19a1	protein_coding	0	0	30369	13	6	367.6264	102.7754	3.576736	13	
218	ENSMUSG00000026126.15	Ptpn18	protein_coding	1.36E-13	3.75E-13	1782	31	20	21.78946	5.877985	3.702364	31	
238	ENSMUSG00000047180.8	Neurl3	protein_coding	1.78E-13	4.90E-13	1369	31	35	22.75947	7.462566	3.047076	31	
239	ENSMUSG00000037447.16	Arid5a	protein_coding	2.53E-08	5.79E-08	1879	31	13	17.74366	5.254115	3.372582	31	
259	ENSMUSG00000050122.18	Vwa3b	protein_coding	8.65E-25	3.12E-24	2541	32	13	39.30092	9.314332	4.21595	32	
306	ENSMUSG00000026072.12	Il1r1	protein_coding	########	########	11983	29	34	162.2162	20.00498	8.105239	29	
308	ENSMUSG00000070942.8	Il1rl2	protein_coding	1.37E-33	5.73E-33	8649	31	1	42.13763	16.94828	2.485372	31	
309	ENSMUSG00000026069.15	Il1rl1	protein_coding	5.82E-43	2.78E-42	1470	31	22	47.56667	8.2869	5.734271	31	
310	ENSMUSG00000026070.15	Il18r1	protein_coding	0.009179	0.014401	184	31	13	8.134531	1.420455	5.693666	31	
311	ENSMUSG00000026068.11	Il18rap	protein_coding	1.39E-29	5.46E-29	834	31	38	36.8258	11.35927	3.239943	31	
313	ENSMUSG00000026062.12	Slc9a2	protein_coding	0.006116	0.009769	966	17	25	7.692649	1.689189	4.533132	17	

Qué haríamos si quisieramos ayudar a los investigadores?

Descarguemos la tabla que se encuentra subida al EVA, conteniendo el material suplementario del artículo.

A	B	C	D	E	F
Supplementary Table 3: Curated cluster id, cell number and annotated cell types together with reference gene markers for annotation.					
Cluster	Cell type	cell number	Markers used for cell type identific	Literature	
1	Connective tissue progenitors	144648	Il1rapl2, Meox2, Tgfb2, Adamts9, P	https://www.ncbi.nlm.nih.gov/pubmed/25249460	
2	Chondrocytes & osteoblasts	132025	Runx2, Twist2, Prrx1	https://www.ncbi.nlm.nih.gov/pmc/articles/PMC4990491/	
3	Intermediate Mesoderm	113083	Wt1, Mylk, Ednra	https://www.ncbi.nlm.nih.gov/pubmed/25480331	
4	Jaw and tooth progenitors	103962	Sox9, Foxp2, Col2a1,Col9a1, Col11a	https://www.ncbi.nlm.nih.gov/pubmed/26969076	
5	Excitatory neurons	97899	Ntng1, Car10	https://www.ncbi.nlm.nih.gov/pmc/articles/PMC4000137/	http://mou
6	Epithelial cells	95672	Epcam, Trp63, Grhl2,	http://www.cell.com/cell/comments/S0092-8674(18)30116-8	https://ww
7	Radial glia	88987	Pth2r, Fabp7, Pax3, Fzd10, Hes5	http://www.cell.com/cell/comments/S0092-8674(18)30116-8	https://ww
8	Early mesenchyme	88546	Gpc5, Smoc1	https://www.ncbi.nlm.nih.gov/pubmed/21194678	https://ww
9	Neural progenitor cells	87150	Prmt8, Gadd45g, Cdkn1c, Btg2	http://www.cell.com/cell/comments/S0092-8674(18)30116-8	https://ww
10	Postmitotic premature neurons	79483	Nkx6-3, Nrn1, Slc17a6, Grem2,	https://www.ncbi.nlm.nih.gov/pubmed/16326147	https://ww
11	Oligodendrocyte Progenitors	76100	Slc17a6, Sox1, Olig2, Nkx2-1	https://www.ncbi.nlm.nih.gov/pmc/articles/PMC3472585/	http://dev.l
12	Isthmic organizer cells	66465	Fgf8, EN2, Fgf15, Fgf17, Pax5	https://www.ncbi.nlm.nih.gov/pubmed/12736208	
13	Myocytes	65733	Neb, Myh3, Tpm2, Acta2 (smooth n	https://www.ncbi.nlm.nih.gov/pubmed/24509862	
14	Neural Tube	64192	Foxb1, Scube2, Prtg	https://www.ncbi.nlm.nih.gov/pubmed/18064677	
15	Inhibitory neurons	61263	Pax2, Slc6a5	http://mousebrain.org/	
16	Stromal cells	60720	Il23a, Bmpr1a, Prtg	https://www.ncbi.nlm.nih.gov/pmc/articles/PMC4307917/	
17	Osteoblasts	51407	Col1a1, Camk1d, Rbm8a	https://www.ncbi.nlm.nih.gov/pubmed/15042706?dopt=Abstract	
18	Inhibitory neuron progenitors	48398	Pax2, Slc6a5	http://mousebrain.org/	
19	Premature oligodendrocyte	45748	Fut9, Id4, Pcdh19, Cdon, Emx1	https://www.sciencedirect.com/science/article/pii/S1567133X06000500	https://ww
20	Endothelial cells	44433	Ptprb, Pecam1, Vwf, Klhl4, Hbegf, E	http://www.cell.com/cell/comments/S0092-8674(18)30116-8	
21	Chondroctye progenitors	42944	ITGA11, ATP1A2, Lamc3, Epha7	http://journals.plos.org/plosone/article?id=10.1371/journal.pone.0082	http://ww
22	Definitive erythroid lineage	75861	Snca, Hbb-bs, Abcb4, Slc4a1, Kel, H	http://www.cell.com/cell/comments/S0092-8674(18)30116-8	https://ww

Supplementary Table 5: Summary of features of all 655 subclusters.

Sub_cluster_i	Sub_cluster_r	Main_cluster_	Main_cluster_	Sub_cluster_r	Sub_trajector	Sub_trajector	Cell_num_E9.	Cell_num_E1(	Cell_num_E1:	Cell_num_E1:	Cell_num_E1:	Average_deve	Total_cells	Minimum_def	Doublet_clust	Detected_dou	Curated_ann	Matched_cell	Matched_cell
cluster.10-1	NA	10	Postmitotic pr	1	NA		21	742	2329	1208	350	11.7417204	4650	NA	Doublet_clust	0.64236559	NA	NA	NA
cluster.10-10	Excitatory neu	10	Postmitotic pr	10	Excitatory neu	29-of-55	10	190	1117	710	334	11.9947056	2361	Iqcj,Robo3,Sir	Not_doublet_	0.02329521	NA	Granule neurc	NA
cluster.10-11	Excitatory neu	10	Postmitotic pr	11	Excitatory neu	7-of-55	3	601	1565	168	9	11.3205456	2346	Grem2,Dlgap2	Not_doublet_	0.00682012	NA	Granule neurc	NA
cluster.10-12	Excitatory neu	10	Postmitotic pr	12	Excitatory neu	19-of-55	2	262	1476	510	78	11.6718213	2328	Tfap2d,Evx2	Not_doublet_	0.01675258	NA	Granule neurc	NA
cluster.10-13	NA	10	Postmitotic pr	13	NA		19	385	1252	506	165	11.6774817	2327	NA	Doublet_clust	0.59948431	NA	NA	NA
cluster.10-14	Excitatory neu	10	Postmitotic pr	14	Excitatory neu	9-of-55	5	524	1431	287	26	11.4142103	2273	Evx1,Skor2	Not_doublet_	0.0074791	NA	Granule neurc	NA
cluster.10-15	Excitatory neu	10	Postmitotic pr	15	Excitatory neu	38-of-55	0	7	386	951	857	12.7076329	2201	Chst1,Prkg2	Not_doublet_	0.01953657	NA	Postmitotic ne	NA
cluster.10-16	Excitatory neu	10	Postmitotic pr	16	Excitatory neu	8-of-55	4	401	1484	156	6	11.3824963	2051	Lect1,Hs3st2	Not_doublet_	0.01462701	NA	Granule neurc	NA
cluster.10-17	Excitatory neu	10	Postmitotic pr	17	Excitatory neu	20-of-55	2	185	1266	411	92	11.7075665	1956	Evx2,Ndst3,H	Not_doublet_	0.02096115	NA	Postmitotic ne	NA
cluster.10-18	Excitatory neu	10	Postmitotic pr	18	Excitatory neu	21-of-55	0	87	1233	477	4	11.7209883	1801	Pdzrn4,Prdm6	Not_doublet_	0.02054414	NA	Postmitotic ne	NA
cluster.10-19	Excitatory neu	10	Postmitotic pr	19	Excitatory neu	12-of-55	6	360	853	271	30	11.4730263	1520	Robo3,Dmbx1	Not_doublet_	0.00460526	NA	Postmitotic ne	NA
cluster.10-2	Excitatory neu	10	Postmitotic pr	2	Excitatory neu	41-of-55	0	17	526	2081	1824	12.7841727	4448	Tfap2d,Hs3st	Not_doublet_	0.01079137	NA	Postmitotic ne	NA
cluster.10-20	Excitatory neu	10	Postmitotic pr	20	Excitatory neu	35-of-55	0	6	445	651	355	12.4299931	1457	Esrrb,Tfap2d	Not_doublet_	0.01304049	NA	Postmitotic ne	NA
cluster.10-21	Excitatory neu	10	Postmitotic pr	21	Excitatory neu	15-of-55	0	77	1174	178	8	11.5814196	1437	Sorcs3,Robo3	Not_doublet_	0.02853166	NA	Postmitotic ne	NA
cluster.10-22	Granule neurc	10	Postmitotic pr	22	Granule neurc	8-of-21	0	71	422	453	421	12.3953914	1367	Samd3,Tspear	Not_doublet_	0.03218727	NA	Granule neurc	CR/Cajal-Retz
cluster.10-23	Excitatory neu	10	Postmitotic pr	23	Excitatory neu	18-of-55	1	99	905	262	20	11.6561772	1287	Otp,Tfap2a	Not_doublet_	0.02874903	NA	Granule neurc	NA
cluster.10-24	Excitatory neu	10	Postmitotic pr	24	Excitatory neu	32-of-55	4	91	426	397	246	12.1786942	1164	Pomc,Atp8b1	Not_doublet_	0.03350515	NA	Granule neurc	NA
cluster.10-25	Excitatory neu	10	Postmitotic pr	25	Excitatory neu	24-of-55	0	119	560	321	60	11.8037736	1060	Sim1,Tmem25	Not_doublet_	0.02358491	NA	Granule neurc	NA
cluster.10-26	Excitatory neu	10	Postmitotic pr	26	Excitatory neu	4-of-55	76	377	435	93	33	11.1351085	1014	Tfap2d,Prss12	Not_doublet_	0.02662722	NA	Granule neurc	NA
cluster.10-27	Excitatory neu	10	Postmitotic pr	27	Excitatory neu	6-of-55	12	138	448	40	3	11.3190328	641	Foxd2	Not_doublet_	0.02028081	NA	Granule neurc	NA
cluster.10-28	Excitatory neu	10	Postmitotic pr	28	Excitatory neu	27-of-55	0	5	276	140	32	11.9392936	453	Slc17a8,Scn9a	Not_doublet_	0.06181015	NA	Granule neurc	NA
cluster.10-29	Excitatory neu	10	Postmitotic pr	29	Excitatory neu	26-of-55	2	11	258	93	45	11.9107579	409	Barhl1,Cacng	Not_doublet_	0.03422983	NA	Granule neurc	NA
cluster.10-3	Excitatory neu	10	Postmitotic pr	3	Excitatory neu	44-of-55	0	1	145	2130	1716	12.8930361	3992	Skor2,Lmx1b,I	Not_doublet_	0.00851703	NA	Granule neurc	NA
cluster.10-4	Granule neurc	10	Postmitotic pr	4	Granule neurc	5-of-21	0	310	2020	935	294	11.8408261	3559	Samd3,Rph3a	Not_doublet_	0.01432987	NA	Granule neurc	NA
cluster.10-5	Excitatory neu	10	Postmitotic pr	5	Excitatory neu	11-of-55	12	650	2277	395	25	11.4318249	3359	Phox2b,Robo3	Not_doublet_	0.00982435	NA	Granule neurc	NA
cluster.10-6	Excitatory neu	10	Postmitotic pr	6	Excitatory neu	17-of-55	1	450	2005	758	80	11.6414693	3294	Robo3,Prdm1(	Not_doublet_	0.02034001	NA	Granule neurc	NA
cluster.10-7	Excitatory neu	10	Postmitotic pr	7	Excitatory neu	23-of-55	2	335	1699	748	143	11.7374445	2927	Vsx2,Tmem13	Not_doublet_	0.01674069	NA	Granule neurc	NA
cluster.10-8	Excitatory neu	10	Postmitotic pr	8	Excitatory neu	28-of-55	3	180	1327	841	334	11.9927374	2685	Sim1,Syndig1	Not_doublet_	0.01638734	NA	Granule neurc	NA
cluster.10-9	Excitatory neu	10	Postmitotic pr	9	Excitatory neu	46-of-55	0	9	55	1385	1194	12.9241392	2643	Robo3,Sv2b	Not_doublet_	0.02762013	NA	Postmitotic ne	CBNBL2/Neur
cluster.1-1	Connective tis	1	Connective tis	1	Connective tis	14-of-16	19	944	10977	23026	30928	12.773257	65894	NA	Not_doublet_	0.01478132	NA	Stromal cell_[	NA
cluster.11-1	Oligodendroc	11	Oligodendroc	1	Oligodendroc	15-of-37	125	1462	2450	593	163	11.3345504	4793	Nkx2-2,Rspo2	Not_doublet_	0.00396411	NA	NA	NA

Introducción a spatial transcriptomics (single cell RNAseq)

Además de tener información de la heterogeneidad del tejido en estudio, nos da información posicional.

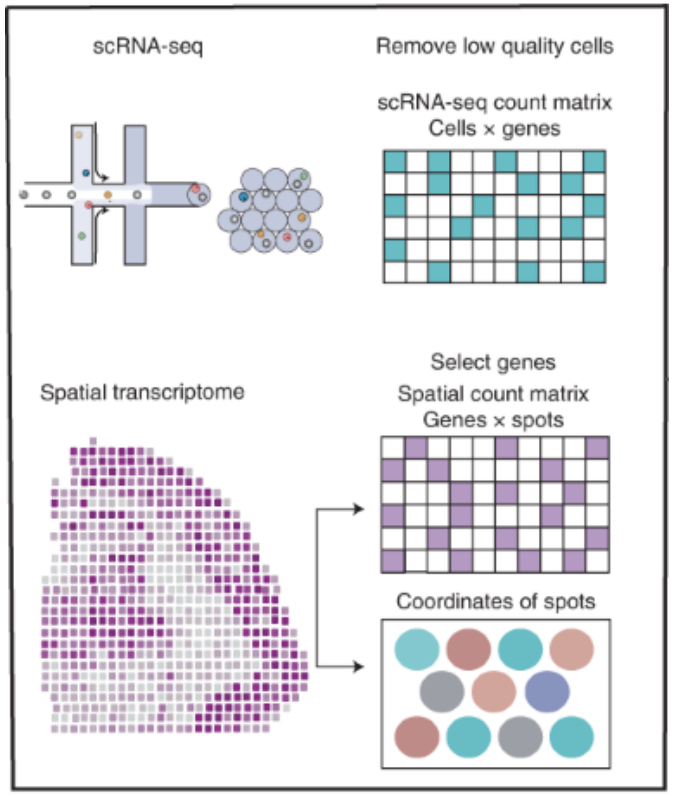

MOSTA Atlas

MOSTA: Mouse Organogenesis Spatiotemporal Transcriptomic Atlas

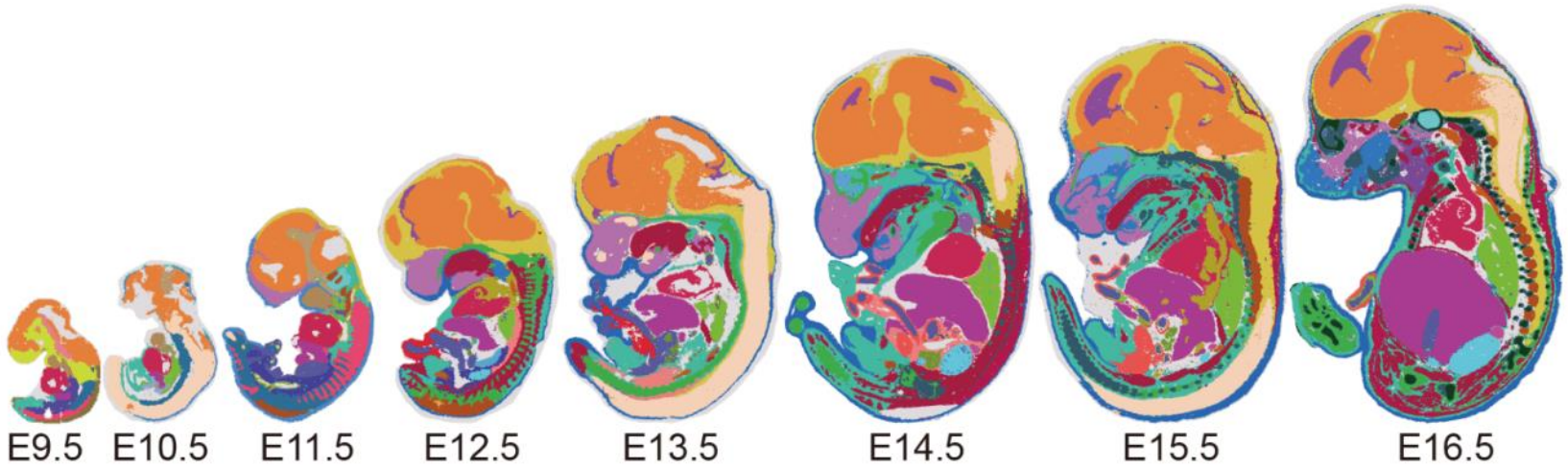

MOSTA database has a total of 53 sagittal sections from C57BL/6 mouse embryos at E9.5 (~7.1 mm2), E10.5 (~11.5 mm2), E11.5 (~18.8 mm2), E12.5 (~32.1 mm2), E13.5 (~48.4 mm2), E14.5 (~64.1 mm2), E15.5 (~70.8 mm2) and E16.5 (~76.1 mm2) using Stereo-seq. For E9.5-E15.5 stages, four to six sections were included from different replicates. As for E16.5, 17 sagittal sections were profiled from two biological replicates, with 13 sections from one single embryo, allowing coverage of all major organs/tissues. In the MOSTA, we provide the spatial map showing the gene expression, gene co-expression modules and regulons in each embryo sagittal sections. Our panoramic atlas will allow in-depth investigation of longstanding questions concerning mammalian development.

Spatial clustering

Search for the annotation, gene expression, gene co-expression modules and regulons in each sagittal mouse embryo section.

Stereo-seq

Protocol of the Stereo-seq chip generation and library preparation.

Resource

We have made our raw data and software resource available for analyse the raw data for the research community.

Download

We provided our processed data and meta data available for the research community.